GEOLOGICA CARPATHICA, 44, 3, BRATISLAVA, JUNE 1993
143 - 153

ENCLAVES AND FAYALITE-BEARING PEGMATITIC "NESTS" IN THE UPPER PART OF THE GRANITE INTRUSION OF THE VELENCE MTS., HUNGARY

GYÖRGY BUDA

Department of Mineralogy, Eötvös L. University, Múzeum krt. 4/A, 1088 Budapest, Hungary

(Manuscript received August 11, 1992; accepted in revised form December 16, 1992)

Abstract: Along the Balaton-Velence fault zone there are a few hypabyssal, small, Variscan (280 mil.years) S-type granitic intrusions. Only one outcrop on the surface is in the Velence Mts. This monzogranite crystallized from a nearly eutectic water-saturated melt at approximately 680 °C, 200 MPa. The granite contains basic magmatic enclaves, metapelitic xenoliths, and fayalite-bearing pegmatitic nests. The basic enclaves represent a primitive magma, with evidence of alteration by the enclosing granitic melt. The metapelitic xenoliths were embedded from the former andalusite hornfels, recrystallized and partially fused in the granitic melt at a pressure and temperature similar to the enclosing granite. The fayalite-bearing pegmatitic nests crystallized at lower temperature (540 °C, 200 MPa) in the upper part of the granite intrusion. Due to the falling temperature and metapelitic xenoliths, locally the oxygen fugacity decreased and quartz, fayalite and K-feldspar crystallized instead of annite-rich biotite.

Key-words: enclaves, fayalite-pegmatite, hypabyssal granite, Hungary (Velence Mts.).

Introduction

In Transdanubia, north of Lake Velence, an intrusive body of Variscan (280 Ma) monzogranite outcrops along the Velence-Balaton fault zone. A basic differentiate (quartz diorite) of the granite occurs in the lower level of the intrusive body penetrated by drilling at Dinnyés. The granite body is transected by granite porphyry and aplite dykes (Fig. 1). The basic differentiate crystallized from a relatively higher-temperature, water-undersaturated melt, whereas the granite crystallized from a low-temperature (680 °C), water-saturated, eutectic melt (Buda 1981, 1985). The intrusion is surrounded by a contact thermal aureole (andalusite hornfels, spotted slate). Near the contact, in the coarse-grained biotite-orthoclase monzogranite, three groups of enclaves have been identified (nomenclature according to Didier 1973):

1 - microgranular quartz monzodioritic enclaves;

2 - surmicaceous, small, lenticular metapelitic xenoliths;

3 - angular, quartzofeldspathic, aplitic congeneric enclaves originating from the marginal part of the intrusion.

The coarse-grained, quartz-, feldspars- and Fe-rich silicate-oxide (fayalite, Fe-amphiboles, Fe-biotite, magnetite) bearing pegmatitic nests occur together with these enclaves, marking the marginal zone of the intrusion.

Analytical procedure

Most of the analyses were performed on an ICXA-733 type electron microprobe with WDS (acceleration voltage 20 kV, sample current 40 - 60 nA) at the Hungarian Academy of Sciences. Plagioclase data in Tab. 1 and fayalite and hornblende data in Tab. 8 were obtained with an AMRAY 18301 Scanning Electron Microscope with EDAX PV9800 EDS (acceleration voltage 20 kV, sample current 1 - 2 nA) at the Department of Petrology and Geochemistry of Eötvös L. University, Budapest.

Table 1: Microprobe analyses of some selected zoned plagioclases from microgranular quartz monzodioritic enclaves.

wt%	1	2	3	4	5	6
SiO_2	49.76	53.87	65.35	53.31	55.36	65.16
Al_2O_3	30.11	27.59	22.13	30.13	28.54	22.19
CaO	16.82	12.67	4.45	12.79	10.37	3.37
Na_2O	3.53	.4.84	8.41	4.25	5.71	9.26
K_2O	0.20	0.32	0.71	0.16	0.20	0.69
Σ	100.42	99.29	101.05	100.64	100.18	100.67
Numbers of ions on the basis of 8(O)						
Si	2.283	2.462	2.853	2.399	2.489	2.855
Al^{IV}	0.717	0.538	0.147	0.601	0.511	0.145
Al^{VI}	0.911	0.948	0.991	0.997	1.001	1.001
Ca	0.827	0.620	0.208	0.616	0.499	0.158
Na	0.314	0.429	0.712	0.370	0.498	0.787
K	0.011	0.018	0.039	0.009	0.012	0.038
Or	0.92	1.69	4.03	0.90	1.19	3.87
Ab	27.24	40.21	74.28	37.19	49.36	80.06
An	71.84	58.10	21.69	61.91	49.45	16.07

Explanations: 1 - core of zoned plagioclase (sample 5900/3); 2 - intermediate zone of the same plagioclase; 3 - rim of the same plagioclase; 4 - inner part of a zoned plagioclase (core was strongly sericitized, sample: 5900/8); 5 - intermediate zone of same plagioclase; 6 - rim of

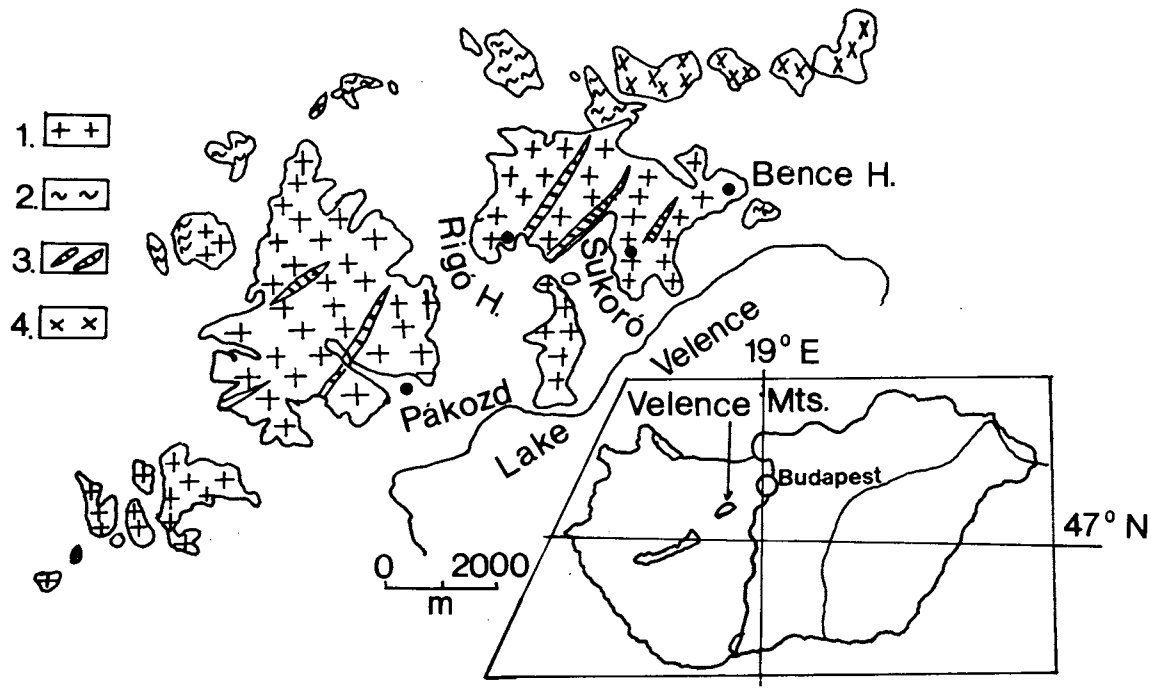

Fig. 1. Geological sketch map of the Velence Mts.
1 - monzogranite; 2 - contact aureole (andalusite hornfels and spotted slates); 3 - granite porphyry and aplite dykes; 4 - andesite

Trace element concentrations were analysed by neutron activation using the Training Reactor of the Technical University, Budapest.

Lithology

Microgranular quartz monzodioritic enclaves

These enclaves, which occur together with the pelitic ones, have been found during geological mapping in the quarry of Rigó Hill (sample No. 5900/3, 5900/8) between Sukoró and Pákozd villages (Fig. 1). They are lenticular, black to dark-grey in colour and their boundaries towards the enclosing granite are diffuse. Some are porphyritic. They contain a considerably smaller amount of biotite than the pelitic xenoliths. Sizes are between 8 - 10 cm. *Plagioclase* is the prevailing constituent, which occurs in large, tabular, euhedral crystals as a porphyritic constituent, or as smaller tabular, lathshaped crystals in a quartz-rich groundmass (Fig. 2a). Both kinds are zoned and most have polysynthetic twins. Frequently, the cores of the crystals are strongly sericitized, sometimes replaced by K-feldspar. The compositions are: cores, An_{72}-An_{62}; intermediate zones, An_{58-49}; outer rims, An_{22-16} (Tab. 1, Fig. 2b). The plagioclase contains abundant acicular apatite crystals. *K-feldspar* is anhedral, occurring together with quartz in the groundmass or replacing plagioclase (Fig. 2c). It has virtually no sodium content. *Quartz* is rounded, and porphyritic, or it forms crystal aggregates, or occurs in the groundmass with K-feldspar as a large anhedral constituent. Plagioclase, biotite, and *amphiboles* "float" in this groundmass. Two main types of amphiboles can be distinguished:

1 - Eu-, or subhedral prismatic crystals, without zonation, which sometimes form aggregates. They are composed of magnesian-hastingsitic hornblende (Tab. 2);

2 - large subhedral or anhedral crystals, frequently zoned and partly replaced by biotite. Iron content increases from the core

Table 2: Microprobe analyses of some selected amphiboles and biotite from microgranular quartz monzodioritic enclaves.

wt%	1	2	3		4
SiO_2	40.56	41.90	44.32	SiO_2	36.20
TiO_2	0.79	1.65	0.32	TiO_2	2.11
Al_2O_3	7.47	9.62	5.93	Al_2O_3	12.49
FeO	28.31	16.81	25.80	FeO	28.89
MnO	1.26	0.38	1.23	MnO	0.54
MgO	5.15	11.17	7.72	MgO	6.55
CaO	10.12	11.28	10.28	CaO	-
Na_2O	3.10	3.57	3.08	Na_2O	0.10
K_2O	0.83	0.78	0.60	K_2O	8.89
Σ	97.59	97.16	99.28	Σ	95.77
Numbers of ions on the basis of 23(O)					22(O)
Si	6.400	6.370	6.725	Si	5.779
Al^{IV}	1.389	1.629	1.060	Al^{IV}	2.221
Fe^{3+}	0.211	0.001	0.215	Al^{VI}	0.130
Al^{VI}	-	0.095	-	Ti	0.253
Ti	0.093	0.189	0.036	Fe	3.857
Fe^{3+}	0.850	0.276	0.814	Mn	0.074
Mg	1.213	2.532	1.747	Mg	1.559
Fe^{2+}	2.675	1.859	2.245	Na	0.032
Mn	0.169	0.049	0.158	K	1.812
Ca	1.710	1.838	1.671		
Na	1.179	1.053	0.905		
K	0.166	1.151	0.117		
Mg/Mg+Fe	0.245	0.543	0.348		

Explanations: 1 - euhedral magnesian-hastingsitic hornblende without zonation (sample: 5900/3); 2 - core of another magnesian-hastingsitic hornblende (sample: 5900/3); 3 - rim of the same hornblende (ferro-edenitic hornblende); 4 - Fe-biotite (sample: 5900/8).

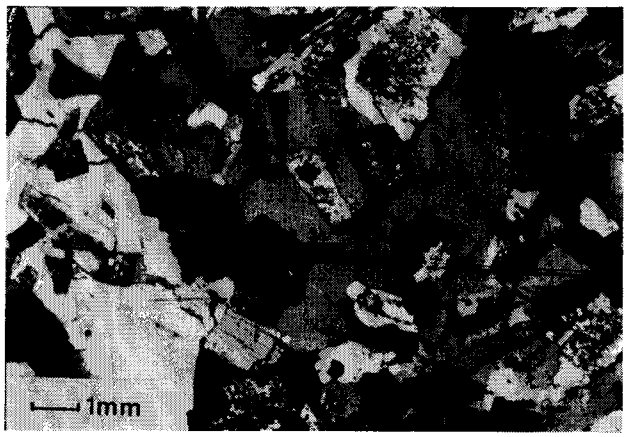

Fig. 2a. Photomicrograph of microgranular quartz monzodioritic enclave (basic zoned plagioclases are "floating" in a groundmass of anhedral quartz and K-feldspar), + N.

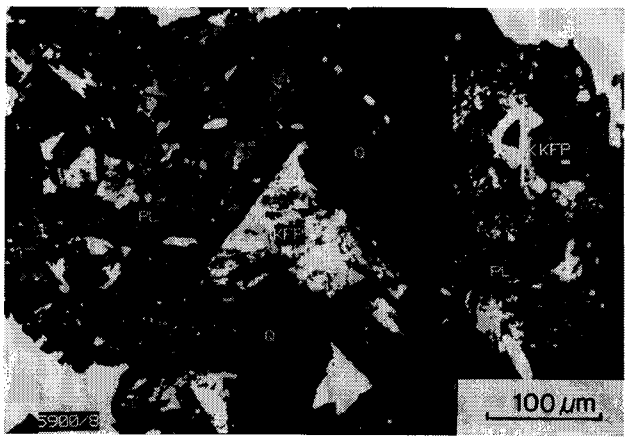

Fig. 2b. Back-scattered electron image of zoned plagioclase in quartz groundmass (An_{72} - An_{55} - An_{22}).

towards the rim (ferro-edenitic hornblende, Tab. 2). The zone boundaries are not well developed. Presumably, the first type crystallized later, when the enclaves were embedded in the granitic melt. Biotite occurs mostly in the groundmass, frequently forming aggregates or replacing amphibole. Its composition is Fe-biotite (Tab. 2), similar to the composition of the biotite of the enclosing granite, but with a slight enrichment of magnesium (Fe/Fe + Mg = 0.78 in granite, 0.71 in enclave). It is supposed that some biotites were formed by K-metasomatic replacement of amphiboles, caused by the enclosing granitic melt. Accessories are *apatite* (acicular, very frequent), *zircon*, and *opaques* (mostly ilmenite, sometimes sphalerite). The enclaves can be classified as quartz monzodiorite on the basis of major elements (Tab. 3). Enrichment of silica, alkalis and iron was most probably caused by the enclosing granitic melt, according to textural evidence. The chondrite-normalised REE distribution is similar to basic igneous rocks, but with a remarkable negative Eu anomaly (Fig. 3). Eu-contents of these enclaves and the enclosing granite are very similar (Eu in enclave: 0.56 g/t and in granite: 0.51 g/t), suggesting that Eu equilibrium was established between the partially fused enclaves and volatile-rich granitic melt at the late stage of differentiation.

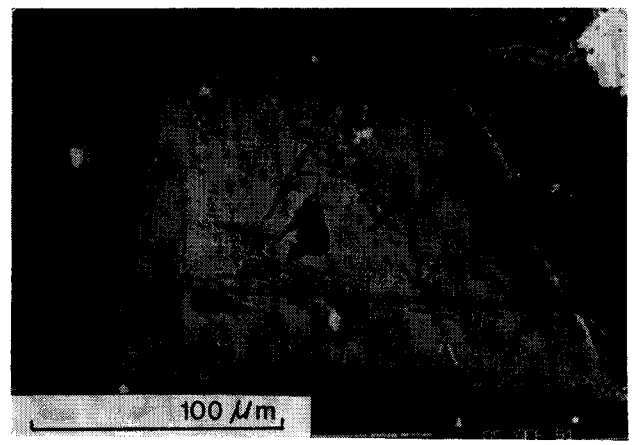

Fig. 2c. Plagioclases (PL) were partly replaced by K-feldspar (KFP) and K-feldspar-quartz (Q) formed the groundmass (BSE).

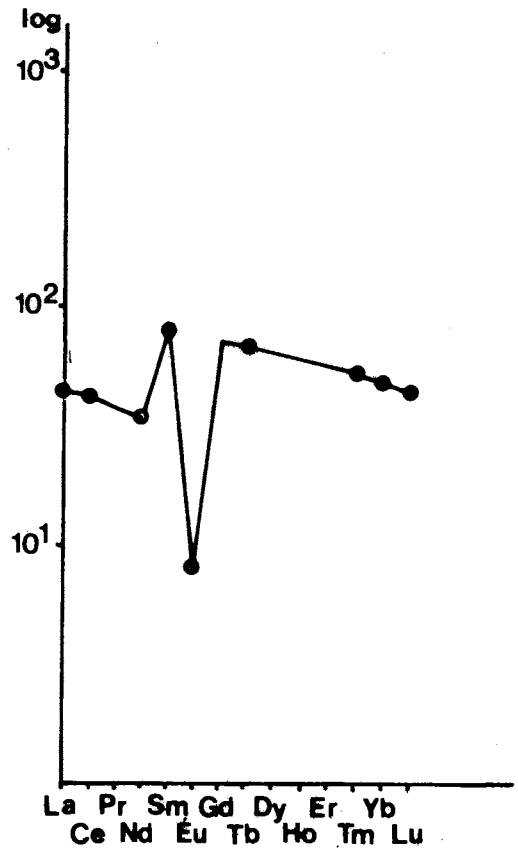

Fig. 3. Chondrite-normalized REE pattern for microgranular quartz monzodioritic enclave.

Surmicaceous metapelitic xenoliths

These xenoliths were first described by Vendl (1914). Many have been found in the quarry of Rigó Hill (sample No. 693/1, 5900/16, 5900/26).

Two types of pelitic xenoliths can be distinguished according to their mineral assemblages, which indicate differences in their silica-content: **1.** andalusite-sillimanite-biotite-feldspars (quartz) xenoliths (silica-rich); **2.** corundum-hercynite-biotite-feldspars xenoliths (silica-deficient).

Table 3: Representative major and trace-element composition of enclave, monzogranite, pegmatitic nest and andalusite hornfels.

wt%	1	2	3	4	5
SiO_2	58.50	73.20	71.00	52.60	74.90
TiO_2	0.90	0.31	0.36	1.05	0.11
Al_2O_3	15.40	13.10	14.80	26.00	13.30
Fe_2O_3	1.44	0.75	0.87	1.32	1.06
FeO	8.25	1.57	2.02	4.68	0.74
MnO	0.25	0.07	0.08	0.14	0.06
MgO	2.16	0.61	0.55	1.78	1.00
CaO	3.28	1.52	1.92	1.69	0.37
Na_2O	4.08	2.86	3.92	2.28	0.15
K_2O	2.37	4.52	3.02	6.00	4.57
P_2O_5	0.17	0.07	0.08	0.10	0.22
H_2O^+	3.41	1.27	1.44	2.14	2.72
H_2O^-	0.18	0.13	0.10	0.02	0.26
CO_2	0.02	0.02	0.05	0.01	0.06
Σ	100.41	100.00	100.21	99.81	99.52
g/t					
La	14.70	41.60	45.90	78.50	50.50
Ce	37.30	77.00	95.60	174.00	119.00
Nd	20.40	27.60	35.00	56.00	41.80
Sm	14.30	8.90	10.90	16.80	10.20
Eu	0.56	0.51	0.51	2.02	1.18
Tb	3.00	1.00	1.30	2.40	1.80
Tm	1.60	0.50	0.60	0.60	1.00
Yb	9.60	2.60	6.90	4.20	5.80
Lu	1.50	0.44	0.96	0.60	0.79
Σ	102.96	160.15	197.67	335.12	232.07
Sc	53.3	4.4	7.5	18.0	9.6
Cr	-	81.3	7.0	120.0	60.0
Co	17.4	3.0	13.6	15.7	20.0
Rb	196.0	215.0	218.0	278.0	166.0
Cs	11.6	4.5	5.1	17.8	10.1
Hf	5.5	3.7	6.2	5.2	5.0
Ta	6.0	1.4	2.9	2.4	1.6
Th	18.7	24.2	35.6	27.7	12.9
U	7.9	5.3	9.1	3.8	4.0
CIPW norms					
Q	10.22	34.49	30.84		
Or	14.00	26.70	17.84		
Ab	34.50	24.18	33.15		
An	12.13	6.04	7.79		
Co	1.67	1.28	2.22		
Et	5.37	1.51	1.36		
Ft	13.95	2.26	2.99		
Mt	2.08	1.08	1.26		
Ap	0.43	0.16	0.18		
Sp	2.20	0.76	0.88		
Σ	96.55	98.46	98.51		

Explanations: 1 - microgranular quartz monzodioritic enclave (sample: 5900/8); 2 - monzogranite (Rigó Hill); 3 - fayalite-bearing pegmatitic nest; 4 - surmicaceous metapelitic xenolith (sample: 693/1); 5 - andalusite hornfels (Bence Hill, sample: 177).

Table 4: Microprobe analyses of some selected feldspars and biotite from metapelitic xenolith.

wt%	1	2	3	4	5	6		7
SiO_2	59.13	61.70	59.12	65.48	65.15	64.21	SiO_2	34.43
Al_2O_3	26.32	24.41	26.63	19.52	19.18	19.91	TiO_2	2.25
CaO	6.88	4.70	6.45	0.04	0.07	0.07	Al_2O_3	22.02
Na_2O	7.36	8.67	7.77	3.23	2.23	2.29	FeO	18.99
K_2O	0.28	0.34	0.30	12.43	14.20	13.85	MnO	0.22
Σ	99.97	99.82	100.27	100.70	100.83	100.33	MgO	6.92
							CaO	0.03
							Na_2O	0.22
							K_2O	9.39
							Σ	94.47
	Numbers of ions on the basis of 8 atoms of oxygen							22(O)
Si	2.636	2.739	2.630	2.967	2.970	2.939	Si	5.270
Al^{IV}	0.364	0.261	0.370	0.033	0.030	0.061	Al^{IV}	2.730
Al^{VI}	1.019	1.016	1.024	1.010	1.001	1.013	Al^{VI}	1.242
Ca	0.329	0.224	0.364	0.002	0.003	0.003	Ti	0.258
Na	0.636	0.745	0.670	0.284	0.197	0.203	Fe	2.425
K	0.015	0.019	0.017	0.719	0.826	0.809	Mn	0.029
Or	1.58	1.92	1.75	71.60	80.51	79.78	Mg	1.570
Ab	64.88	75.40	67.44	28.25	19.15	19.89	Ca	0.005
An	33.54	22.68	30.81	0.15	0.34	0.33	Na	0.065
							K	1.833

Explanations: 1 - core of a zoned, twinned plagioclase (sample: 693/1); 2 - outer zone of the same plagioclase; 3 - average composition of two plagioclases (sample: 5900/16); 4 - orthoclase (sample: 693/1); 5 - orthoclase near to plagioclase No. 1, 2 (sample: 693/1); 6 - orthoclase near to plagioclase No. 3 (sample: 5900/16); 7 - Al-rich biotite (sample: 693/1).

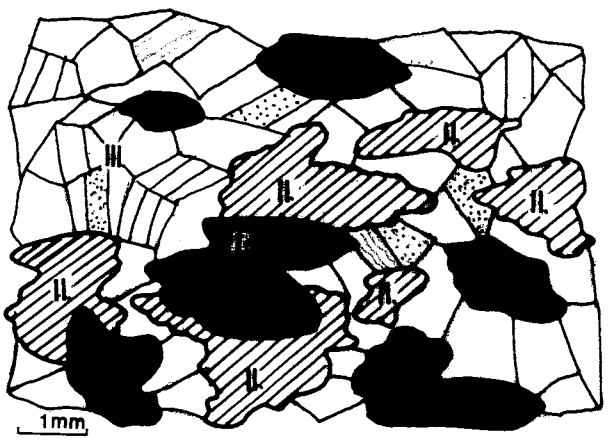

Fig. 4. Texture of a surmicaceous silica- and aluminium - rich xenolith. I - Si-poor spots: biotite, hercynite, corundum, feldspars, ilmenite. II - Si-rich spots: poikiloblastic andalusite, sillimanite, quartz, feldspars, ilmenite, biotite. III - granoblastic leucosome: feldspars, rare quartz, biotite.

These lenticular enclaves have a dark-grey to black colour with a few mm sick, lighter grey bands and lenses (leucosome). Their sizes are variable, but are most commonly 3 - 5 cm. Some of them have oriented, dark-grey to black prismatic spots (pseudomorph after andalusite, Figs.4, 5a) occurring in a fine-

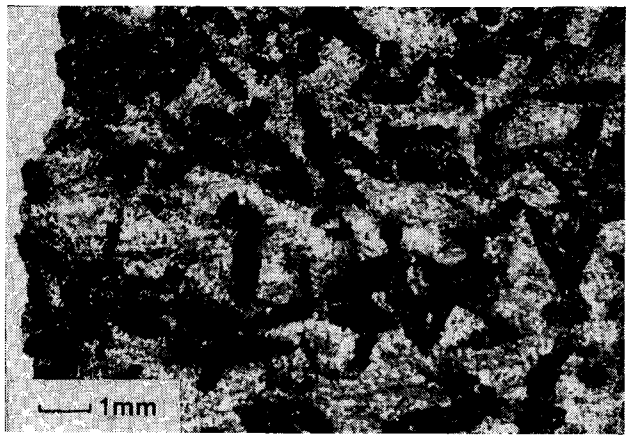

Fig. 5a. Photomicrograph of surmicaceous metapelitic xenolith, 1N (see Fig. 4).

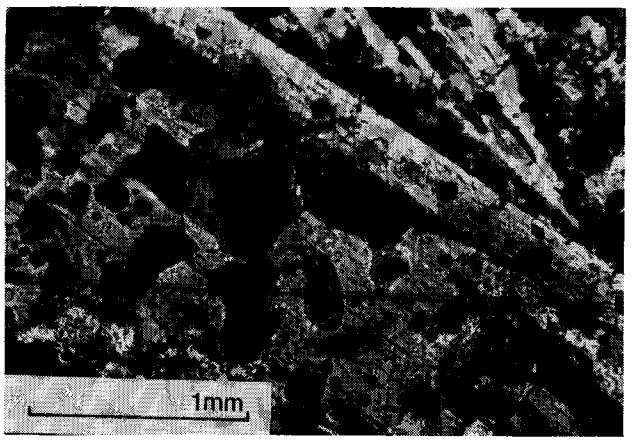

Fig. 5c. Poikiloblastic andalusite integrowth with sillimanite, +N.

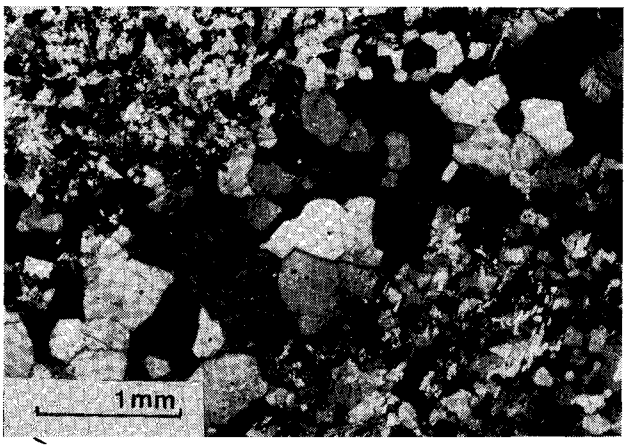

Fig. 5b. Granoblastic band of feldspars and quartz (leucosome), + N.

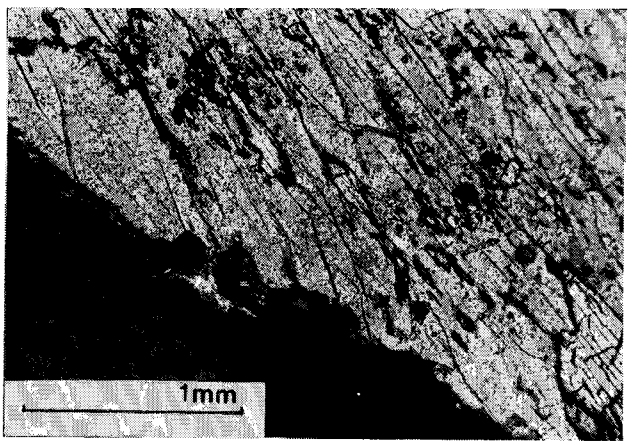

Fig. 5d. Paramorphic replacement of andalusite by sillimanite in metapelitic xenolith, +N.

grained, grey groundmass. *Biotite* is the most common constituent. It is Al-rich (Tab. 4) and strongly pleochroic (reddish and yellowish brown). It is found mostly in the dark-grey spots or it forms oriented bands. A few grains are also observed in the leucosome. Relicts can be observed in sillimanite and corundum, sometimes surrounded by hercynite and ilmenite. Two types of *K-feldspars* can be recognised: 1 - anhedral, which occurs in the interstices of biotite-rich spots, together with sillimanite, andalusite and plagioclase (quartz), without any traces of exsolution of albite. Composition: $Or_{71.6}Ab_{28.3}An_{0.1}$ (Tab. 4); 2 - sub- or euhedral, which forms granoblastic texture in the leucosome (Fig. 5b), sometimes with hair-perthitic albite. Composition: $Or_{80.5}Ab_{19.2}An_{0.3}$ (Tab. 4). There is little 2V and it is orthoclase according to its optical and X-ray properties. The compositional variations are due to the subsolidus segregation of a Na-rich phase, caused by the rate of cooling and volatile enrichment. Plagioclase is sub- or euhedral, untwinned or sometimes polysynthetically twinned, frequently zoned. The compositions are variable between albite and andesine (max: An_{34}, Tab. 4), sometimes partly altered to sericite. *Plagioclase* occurs in the leucosome and in the dark part of enclaves. *Quartz* is very rare, but it sometimes occurs in the granoblastic leucosome. Sillimanite does not occur in every metapelitic enclave. Two textural varieties can be observed: 1 - poikiloblastic, containing hercynite, ilmenite, biotite inclusions or relicts and frequently occurring with andalusite; 2 - elongated, acicular intergrowths with poikiloblastic andalusite (Fig. 5c). Sometimes the acicular crystals transect spots (pseudomorph after early andalusite) where - due to deficiency of silica - they have been transformed to corundum. *Sillimanite* contains a small amount of iron (Tab. 5). *Andalusite* mostly has poikiloblastic texture, containing K- feldspar, biotite and ilmenite inclusions. Sometimes it is pleochroic, especially the core of large crystals. Its composition is normal, with a small amount of iron (Tab. 5). The paramorphic replacement of andalusite by sillimanite is frequent (Fig. 5d, Kerrick 1990; p. 230 - 236). Earlier relicts of andalusite were not observed, but the outline of the biotite-, hercynite-, corundum-, feldspars-, ilmenite-bearing aggregates (Figs. 4, 5a) suggest that they originated from andalusite that was transformed into this mineral assemblage through partial fusion of other constituents, caused by the thermal effect of the granitic melt. *Corundum* occurs mostly in the silica-deficient metapelitic xenoliths, as anhedral or subhedral crystals. It is observed in biotite-rich spots, but can also be found in the leucosome. Sometimes it replaces sillimanite in the Si-deficient environment. It is sometimes pleochroic (ε'=light-blue, ω'=dark-blue). *Hercynite* is rather frequent and occurs in every metapelitic xenolith. It forms large eu- or subhedral, darker green crystals in the Si- deficient varieties. In silica-rich varieties, it is usually smaller, sub- or anhedral, and light-green in colour. Some grains contain a small amount of

Table 5: Microprobe analyses of some selected sillimanite, andalusite, ilmenite and hercynite from metapelitic xenolith.

wt%	1	2		3		4	5
SiO_2	37.13	36.85	TiO_2	51.20	TiO_2	0.02	0.06
Al_2O_3	62.29	62.09	FeO	38.61	Al_2O_3	59.30	59.18
Fe_2O_3	0.43	0.38	MnO	9.05	Cr_2O_3	-	0.39
Σ	99.85	99.32	Σ	98.86	FeO	37.57	36.64
					MnO	0.89	0.57
					MgO	3.01	3.99
					Σ	100.79	100.83
	20 oxygen		6 oxygen			32 oxygen	
Si	4.016	4.008	Ti	1.976	Ti	0.008	0.008
Al	7.944	7.960	Fe	1.654	Al	15.816	15.784
Fe^{3+}	0.036	0.032	Mn	0.394	Cr	-	0.072
					Fe	7.096	6.880
					Mn	0.168	0.112
					Mg	1.016	1.336

Explanations: 1 - sillimanite (sample: 5900/16); 2 - andalusite (sample: 5900/16); 3 - ilmenite (sample euhedral: 5900/26); 4 - hercynite (sample: B-5); 5 - hercynite (sample: 5900/26).

chromium. Its average composition is $Hc_{83.8}$; $Sp_{14.1}$; $Gal_{1.7}$; $Cr_{0.4}$ (Tab. 5). *Ilmenite* is very frequent, rather small, eu- and anhedral. The rounded crystals of ilmenite, together with xenotime, monazite, and zircon, are arranged along well-defined lines, most probably marking the original depositional bedding. In contrast, the larger euhedral grains occurring near or in biotite, formed during decomposition of biotite caused by the heat of the granitic melt. In some xenoliths, only ilmenite occurs but in some others nearly every ilmenite is intergrown with rutile. Mn-content of secondary ilmenite is high (MnO = 9.05 wt%, Tab. 5) suggesting an increase of oxygen fugacity due to higher temperature. *Monazite* is very small, rounded, and mostly less than 10 μm. It can be found together with zircon, xenotime and ilmenite having similar grain sizes. Most probably they have a detrital origin. They are responsible for the high REE enrichments of the xenolith (Tabs. 3, 6 - Fig. 6), based on the La, Ce, Nd and Sm ratios in the monazite and in the whole rock (average: 1.4×10^5). Beside Ce, monazite contains higher amounts of La, Nd, Th, U, and some Pr, Sm, Gd, Y, and Ca (Tab. 6). *Zircon* is eu-, sub- and anhedral (rounded), rather frequently zoned. Sometimes it is intergrown with xenotime. It can also be observed in biotite, where it is surrounded by a wide pleochroic halo. *Xenotime* is slightly smaller than monazite; it forms either separated rounded grains or intergrowths with zircon. It is probably of detrital origin. It contains 2 - 7 wt% Gd, Dy, Er, and Yb, (Tab. 6, Fig. 6). The HREE enrichment of the xenoliths is due to xenotime.

The major element compositions of metapelitic xenoliths (Tab. 3) are similar to the average composition of marine pelitic rocks. Significant differences in the water, sodium, and potassium content can be attributed to dewatering and perhaps a slight effect from the enclosing granitic melt.

The considerable enrichment of REE (Tab. 3) results from the accessories (monazite, xenotime, zircon). Similar enrichment was described by Price (1983) in sillimanite-biotite-muscovite resistites of S-type Koetong granites (Australia). Monazite is the main source of LREE, based on similar light lanthanide ratios in monazite and in the whole xenolith (in monazite: La/Ce=0.47, Ce/Nd=2.5, La/Nd=1.20, in xenolith: 0.45, 3.1, 1.40). Th and U are most probably enriched in both monazite and zircon. Xenotime is the carrier of HREE. Chondrite-normalized (Haskin et al. 1968) REE distribution in the contact andalusite-hornfels is very similar to the xenoliths (Fig. 6) and ratios of light lanthanides are nearly the same (La/Ce=0.46, Ce/Nd=3.1, La/Nd=1.42), supporting the idea that the xenoliths originated from the former contact aureole.

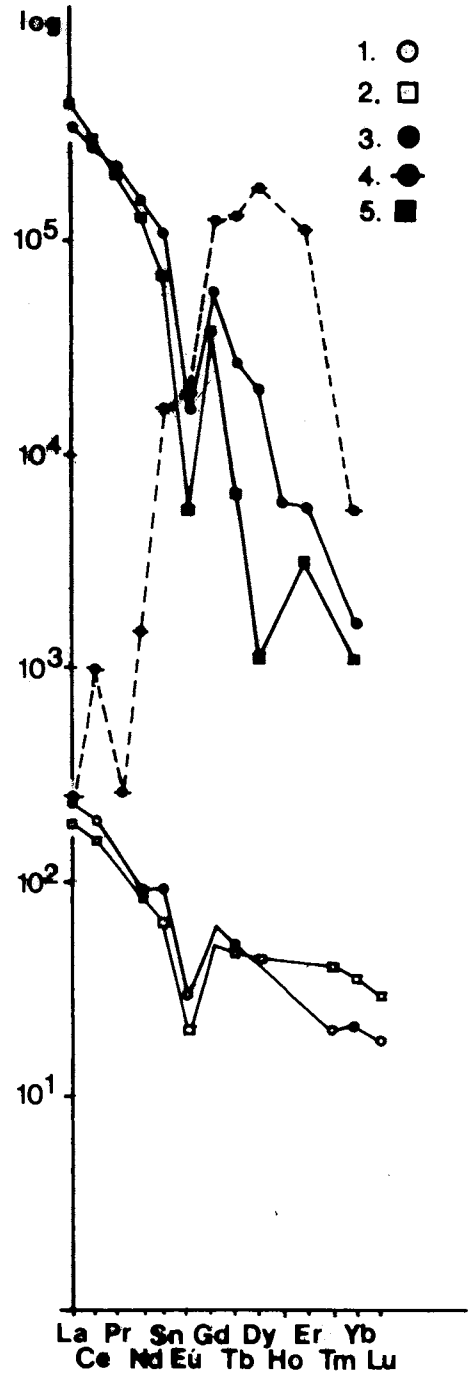

Fig. 6. Chondrite-normalized REE patterns for surmicaceous metapelitic xenolith, andalusite hornfels and their accessories.
1 - surmicaceous metapelitic xenolith (Rig6 Hill); 2 - andalusite hornfels (Bence Hill); 3 - monazite from surmicaceous metapelitic xenolith (Rig6 Hill); 4 - xenotime from surmicaceous metapelitic xenolith (Rig6 Hill); 5 - monazite from andalusite hornfels (Bence Hill).

Table 6: Microprobe analyses of monazite and xenotime from metapelitic xenolith and andalusite hornfels.

wt%	1	2	3*	4*
La_2O_3	13.37	18.17	15.13	0.01
Ce_2O_3	28.29	31.34	28.69	0.10
Pr_2O_3	3.00	2.86	2.50	0.06
Nd_2O_3	11.29	9.02	8.62	0.10
Sm_2O_3	2.33	1.43	1.35	0.34
Eu_2O_3	0.12	0.48	0.33	0.15
Gd_2O_3	1.63	1.01	1.15	3.48
Tb_2O_3	0.14	0.02	0.11	0.69
Dy_2O_3	0.77	0.33	0.55	6.72
Er_2O_3	0.13	0.08	0.06	3.58
Yb_2O_3	0.04	0.00	0.00	2.55
Y_2O_3	2.72	2.06	2.47	40.66
ThO_2	3.99	0.29	4.86	0.77
UO_2	1.47	0.29	0.30	0.78
CaO	0.94	0.57	1.31	0.12
P_2O_5	30.12	30.18	29.62	32.81
Σ	100.35	98.13	97.05	92.92
	Numbers of ions on the basis of 16 oxygen			
La	0.769	1.054	0.890	0.001
Ce	1.615	1.804	1.675	0.005
Pr	0.171	0.164	0.145	0.003
Nd	0.628	0.507	0.491	0.005
Sm	0.126	0.078	0.074	0.017
Eu	0.006	0.026	0.018	0.007
Gd	0.085	0.052	0.061	0.166
Tb	0.007	0.001	0.006	0.032
Dy	0.039	0.017	0.029	0.311
Er	0.006	0.004	0.003	0.162
Yb	0.002	0.000	0.000	0.112
Y	0.226	0.173	0.210	3.111
Th	0.142	0.010	0.176	0.025
U	0.051	0.010	0.011	0.025
Ca	0.157	0.096	0.223	0.018
P	3.976	4.018	4.000	3.993
ΣLREE/U+Th	13.56	180.4	17.51	0.62
ΣLREE/Y	14.64	20.85	15.60	-

Explanations: 1 - monazite from metapelitic xenolith (average of 4 grains, 693/1); 2 - monazite from andalusite hornfels (Th-poor variety, Bence Hill, sample: 177); 3* - monazite from andalusite hornfels (richer in Th, Ca, poorer in La, Bence Hill, sample: 177); 4* - xenotime from metapelitic xenolith (sample: 693/1). *Semiquantitative composition due to small grain sizes (less than 10 μm).

Fayalite-bearing pegmatitic "nests"

The coarse-grained pegmatitic nests are 15 - 25 cm in diameter and occur together with the above-mentioned enclaves. The middle of the "nest" contains coarse-grained, pinkish K- feldspar, grey quartz, large, flaky, black or greenish biotite and brown to greenish-brown, anhedral or prismatic euhedral fayalite. The coarse-grained core is surrounded by a zone of equigranular feldspars, quartz, and biotite and a 2 - 3 cm wide,

Table 7: Microprobe analyses of plagioclase and K-feldspar from fayalite-bearing pegmatitic nest.

wt%	1	2	3	4	5	6
SiO_2	62.91	62.61	63.90	63.99	68.40	65.87
Al_2O_3	23.71	23.39	22.67	22.55	19.66	19.06
CaO	4.44	4.49	3.54	3.42	0.07	0.14
Na_2O	8.37	8.59	8.91	9.30	10.55	1.87
K_2O	1.00	0.72	0.79	0.76	0.12	13.65
	100.43	99.80	99.81	100.02	98.80	100.59
	Numbers of ions on the basis of 8 atoms of oxygen					
Si	2.777	2.781	2.827	2.828	3.008	2.992
Al^{IV}	0.223	0.219	0.173	0.172	-	0.008
Al^{VI}	1.011	1.004	1.010	1.003	1.019	1.013
Ca	0.210	0.214	0.168	0.162	0.003	0.007
Na	0.716	0.739	0.764	0.796	0.898	0.165
K	0.056	0.041	0.044	0.043	0.007	0.791
Or	5.74	4.09	4.51	4.28	0.77	82.14
Ab	72.86	74.40	78.29	79.54	98.90	17.13
An	21.40	21.51	17.20	16.18	0.33	0.73

Explanations: 1 - plagioclase without zoning; 2 - inner part of a slightly zoned plagioclase; 3 - outer part of the same plagioclase; 4 - another plagioclase; 5 - rim of the same plagioclase; 6 - K-feldspar.

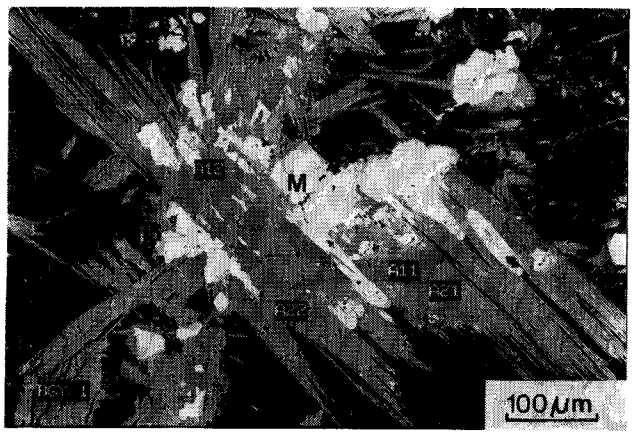

Fig. 7. Back-scattered electron images of acicular grunerite (A11, 12, 21, 22) and magnetite (M) in altered fayalite (iddingsite).

biotite-rich outer rim. K-feldspar is the prevailing constituent, mostly anhedral, sometimes hair-perthitic, with plagioclase and biotite inclusions. Composition: $Or_{82}Ab_{17}An_1$ (Tab. 7). It always contains an albitic phase according to X- ray powder diffraction investigation; the (131) peak splits into a higher and a lower intensity peak, indicating triclinic domains in structure (triclinicity: 0.56, intermediate microcline). According to the Evans et al. (1963) least- squares-refinement unit-cell counting, the triclinic model is not convergent, which suggests a prevailing monoclinic phase beside the triclinic one. *Plagioclase* is eu- or subhedral with polysynthetic twins, slightly zoned, with sericitized cores. Composition: An_{22-16}, outer rim is albite (Tab. 7). *Quartz* is coarse-grained, sub- or euhedral, containing abundant fluid inclusions (see below). *Fayalite* is an- or euhedral. The euhedral

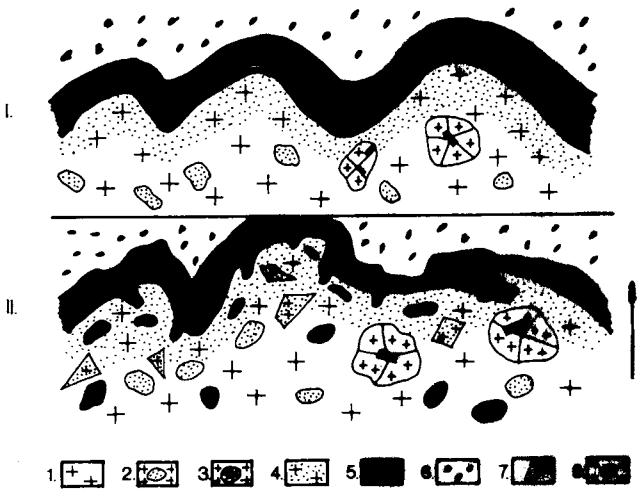

Fig. 8. Ideal sections of the two successive stages of granitic intrusion (I. and II.).
1 - biotite orthoclase monzogranite; 2 - microgranular quartz monzodioritic enclaves; 3 - fayalite-bearing pegmatitic nests; 4 - fine-grained aplite-like margin of intrusion; 5 - andalusite hornfels; 6 - spotted slates; 7 - quartzofeldspathic, aplitic, congeneric enclaves; 8 - surmicaceous metapelitic xenolith.

crystals are large, prismatic (l =6 mm, w =4 mm), slightly pleochroic (pinkish), $2V_\alpha=53°$ (Fo_7). It contains inclusions of euhedral magnetite, rounded quartz, biotite, and hornblende. Around the magnetite, flaky or acicular grunerite can be observed, both of which are enriched towards the rim of fayalite. Unit-cell parameters calculated from X-ray powder patterns (Siemens D500 diffractometer, CuK_α radiation, Si internal standard) are: a=4.8185(6)Å, b=10.475(2)Å, c=6.0908(9)Å, d_{130obs}=2.829Å, $d_{130calc}$=2.826Å. The composition is Fo_6, according to the Yoder & Sahama (1957) and Fischer & Medaris (1969) methods. It contains a considerable amount of manganese, as measured by microprobe: $Fo_9Fa_{86}Te_5$ (Tab. 8). Very frequently they have been altered to green or reddish- brown iddingsite. Two types of grunerite can be distinguished: **1** - acicular, interference colour 2nd order blue, $\gamma/c=16°$ very slightly pleochroic. The rims of the crystals are slightly richer in iron than the cores. Usually they occur near the rim of fayalite, associated with magnetite (Fig. 7); **2** - sheaf-like with wavy extinction; they always surround euhedral magnetite in fayalite. The first type is richer in magnesium than the second one (Tab. 8).

Two types of iddingsite exist: **1** - greenish; **2** - reddish-brown. Both are alteration product of fayalite; sometimes fayalite is completely altered to iddingsite (Tab. 8). *Biotite* occurs in, or near, fayalite. Biotite is strongly pleochroic and sometimes zoned. The cores of crystals are reddish-brown to yellowish-brown with Ti-, Fe-enrichment, whereas the rim is green or light-brown, having a lower titanium content (Tab. 8). *Hornblende* is large, eu- or subhedral, and strongly pleochroic (γ'=bluish green, X_α' = yellowish green). The rims of crystals are frequently altered to biotite. Its composition is ferro-hornblende (Tab. 8). The distribution of Ca within one crystal is uneven. Pyrite is very rare and anhedral.

The chemical composition is similar to that of the enclosing granite (Tab. 3). A slight REE enrichment can be observed, HREE enrichment (Yb) is probably due to an increasing amount of solutions at the final stages of crystallization. Heavy

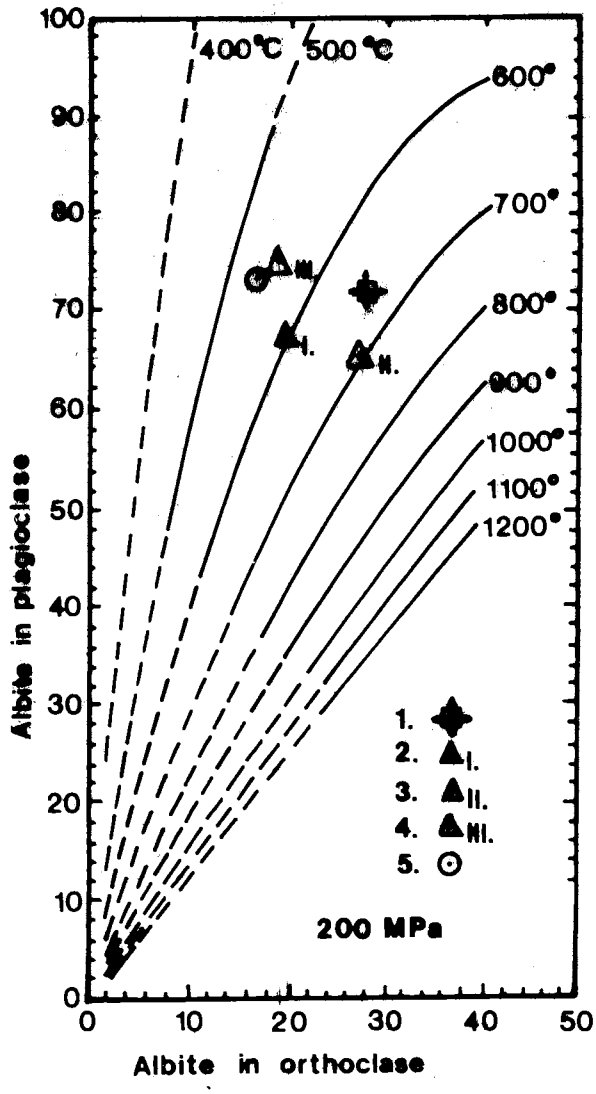

Fig. 9. Determinative curves for temperatures of crystallization of coexisting feldspars (Stormer 1975) from granite, xenolith and pegmatitic "nests".
1 - monzogranite (Ab in Or: 28±2 mol%, Ab in Pl: 72±2 mol%, temperature: 676 °C±32 °C, Buda (1985), calculated using sanidine-microcline solid-solution parameters); 2 - (I) leucosome in metapelitic xenolith, (sample 5900/16, Ab in Or: 20 mol%; Ab in Pl: 67 mol%, temperature 600 °C); 3 - (II) leucosome in metapelitic xenolith (sample 693/1, core: Ab in Or: 28 mol%, Ab in Pl: 65 mol%, temperature 690 °C); 4 - (III) leucosome in metapelitic xenolith (sample 693/1, rim: Ab in Or: 19 mol%, Ab in Pl: 75 mol%, temperature: 550 °C); 5 - fayalite-bearing pegmatitic nest (Ab in Or: 17 mol%, Ab in Pl: 73 mol%, temperature 540 °C).

lanthanides form complexes with CO_3^{2-}, SO_4^{2-} and PO_4^{3-} and precipitate after light lanthanides, consequently they are enriched at the latest stage of crystallization and probably remain in the fluid inclusions of quartz.

Andalusite hornfels

Andalusite hornfels occurs at the contact of the granite (sample No. 177) intrusion. Quartz is the prevailing constituent, occurring as coarse- and fine-grained forms. The latter is a se-

Table 8: Microprobe analyses of fayalite, amphibole, biotite and iddingsite from pegmatitic nest.

wt%	1	2		3	4		5		6	7	8
SiO_2	30.60	30.10	SiO_2	47.67	46.73		43.33	SiO_2	35.49	36.34	44.31
Al_2O_3	-	0.43	Al_2O_3	0.73	0.92		7.81	TiO_2	2.96	0.51	-
FeO	63.20	62.30	FeO	39.80	41.29		29.91	Al_2O_3	12.83	12.51	-
MnO	3.42	3.47	MnO	3.72	3.96		1.15	FeO	29.69	30.76	39.20
MgO	3.57	3.86	MgO	5.77	4.30		4.87	MnO	0.55	0.66	0.50
CaO	0.10	0.13	CaO	0.47	0.48		9.30	MgO	5.73	6.64	1.11
Σ	100.89	100.29	Σ	98.16	97.68	Na_2O	1.59	CaO	-	-	1.56
						K_2O	0.39	Na_2O	0.22	0.15	-
						Σ	98.35	K_2O	8.97	8.76	0.05
								Σ	96.44	96.33	86.73
				Numbers of ions on the basis of-							
	8 atoms of (O)			23 atoms of (O)				22 atoms of(O)			
Si	1.001	0.987	Si	7.711	7.682		6.567	Si	5.664	5.839	
Fe	1.725	0.016	Al^{IV}	0.139	0.178		1.395	Al^{IV}	2.336	2.161	
Mn	0.095	1.709	Fe^{3+}	0.150	0.140		0.038	Al^{VI}	0.079	0.155	
Mg	0.174	0.096	Al^{VI}	-	-		-	Ti	0.354	0.061	
Ca	0.003	0.188	Fe^{3+}	0.505	0.540		1.792	Fe^{2+}	3.956	4.125	
Al	-	0.004	Mg	1.389	1.054		1.100	Mn	0.075	0.084	
Fo =	8.7	9.4	Fe^{2+}	3.106	3.406		1.961	Mg	1.363	1.590	
Te =	4.8	4.8	Mn	-	-		0.147	Ca	-		
Fa =	86.5	86.8	Fe^{2+}	1.624	1.591		-	Na	0.067	0.047	
			Mn	0.511	0.551		0.001	K	1.827	1.795	
			Ca	0.082	0.083		1.510				
			Na	-	-		0.467				

Explanations: 1 - fayalite (measured with WDS, JEOL); 2 - fayalite (measured with EDS, AMRAY); 3 - Fe-Mn-Mg amphibole, grunerite (acicular); 4 - Fe-Mn-Mg amphibole, grunerite (sheaf-like); 5 - ferro-hornblende; 6 - biotite with brown pleochroism; 7 - biotite with green or light brown pleochroism; 8 - iddingsite (reddish-brown).

gregation showing granoblastic texture. Poikiloblastic biotite, muscovite and andalusite and granoblastic quartz are newly formed minerals caused by the thermal effect of the granite intrusion. This association can coexist at about 550 °C, around 200 MPa pressure (hornblende- hornfels facies). Monazite, xenotime, zircon, rutile, ilmenite and pyrite are the most important accessories. Two monazite varieties can be distinguished: **1.** Th-Ca-poor; **2.** Th-Ca-rich (Tab. 6). Sometimes they are zoned, with the outer zone richer in Th and U than the core. Xenotime is mostly smaller than monazite (below 10 μm) and contains a higher amount of U and Th. Zircon is bigger than 10 μm, mostly rounded. The above-mentioned minerals, together with ilmenite (occur in chloritized biotite or in muscovite) are most probably detrital in origin. The acicular rutile and pyrite are secondary minerals. The rock is enriched in silica and potassium due to the presence of quartz-rich granoblastic segregates that alternate with pelitic bands (Tab. 3). The REEs are enriched and show similar chondrite-normalised patterns to the metapelitic xenoliths (Fig. 6). REE enrichments are due to the detrital monazite, xenotime, etc.

Summary and conclusions

We can extract information about the physical-chemical condition of the granitic magma during crystallization, and the mechanism and level of intrusion in the earth's crust from the enclaves and pegmatitic "nests". The microgranular basic enclaves formed from a relatively primitive magma (undifferentiated REE distribution, high An-content, etc.), derived from may have partially melted upper mantle, which initiated partial fusion of the crust to produce a granitoid melt. The enclosing granitic melt altered the original composition of the enclaves, causing enrichment in Si and alkalies, and Eu equilibrium. The metapelitic xenoliths, together with angular quartzofeldspathic, aplitic enclaves, were embedded in the granitic melt in the latest stage of granite intrusion (Fig. 8), deduced from similar accessory minerals in enclaves and in hornfels (monazite, xenotime, zircon etc.), from texture, and from pT conditions of newly formed minerals in the enclaves. Temperature of the granitic melt at the late stage of crystallization was about 680 °C at 200 MPa, based on two-feldspar thermometry (Stormer 1975; Whitney & Storme 1977; Fig.9), biotite stability (Wones & Eugster 1965; Wones 1972; Fig.10) and the eutectic crystallization temperature of feldspars and quartz (Winkler & Breitbart 1978). The new minerals were formed in fragments of hornfels embedded in the granitic melt according to the following reactions:

silica-rich part of hornfels (1)
biotite + quartz → sillimanite (andalusite) + hercynite + orthoclase + ilmenite + water

silica-deficient environment (2)
biotite + andalusite → corundum + hercynite + orthoclase + ilmenite + water.

High Al-content of biotite and early andalusite are responsible for the formation of Al-rich minerals. The liberated volatiles played an important role in partial fusion.

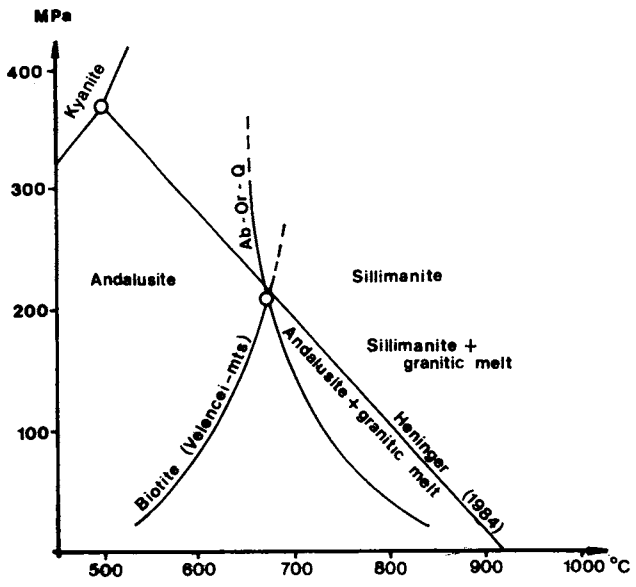

Fig. 10. Phase equilibrium diagram of Al_2SiO_5 polymorphs, biotite stability of the granite of Velence Mts. (based on Fe/Fe+Mg=0.78 ratio, HM buffers) and Ab-Or-Q stability as functions of pressure and temperature. Triple point according to Holdaway (1971). Ab-Or-Q minimum melting curve according to Tuttle & Bowen (1958).

Coexistence of andalusite with sillimanite in a partially fused melt having granitic composition (Fig. 10) suggests the same pT conditions that were determined for the enclosing granite. This conclusion is also supported by two feldspar thermometry (550 - 690 °C, 200 MPa; Fig. 9). The lower temperatures resulted from a solid-state exsolution promoted by enrichment of volatiles.

In pegmatitic nests, oxygen fugacities dropped drastically as a result of metapelitic environment and radical temperature decrease from 680 °C to 540 °C (Fig. 9), so instead of Fe-rich biotite, fayalite crystallized (Fig. 11) in the uppermost part of the intrusion, according the equation (Eugster & Wones 1962):

biotite + quartz → orthoclase (microcline) + fayalite + water

Volatile enrichment increased the oxygen fugacities through the dissociation of water. Therefore, magnetite-grunerite formed in fayalite, followed by extensive iddingsitisation. According to fluid inclusion studies, the secondary liquid-gaseous inclusions in the quartz formed at 400 °C at presumed 200 MPa pressure in healed fractures (Gatter & Molnar 1992). At the contact zone, a new mineral assemblage formed due to the thermal effect of the granite intrusion. This assemblage (muscovite+biotite+andalusite) can coexist at 550 °C, 200 MPa.

According to Jaeger (1957, 1961, 1964) only a part of the heat of granitic magma can be transmitted to surrounding country rocks. The higher temperature mineral assemblage of the contact suggests higher temperature conditions in the crust before intrusion, which can provide a basis for estimating a depth of intrusion, of about 4 - 5 km.

Acknowledgements: I thank the Hungarian National Science Foundation (OTKA) for its generous support of this study with grant No. 2299, I also thank Dr. G. Nagy, Dr. G. Dobosi, K. Török and M. Jánosi for the microprobe analyses and Dr. Gy. Lovas for X-ray calculations. The author is indebted to the late Dr. J. Bérczi for completing the NAA analyses. I thank Dr. W. Heins for critical reviews of the manuscript.

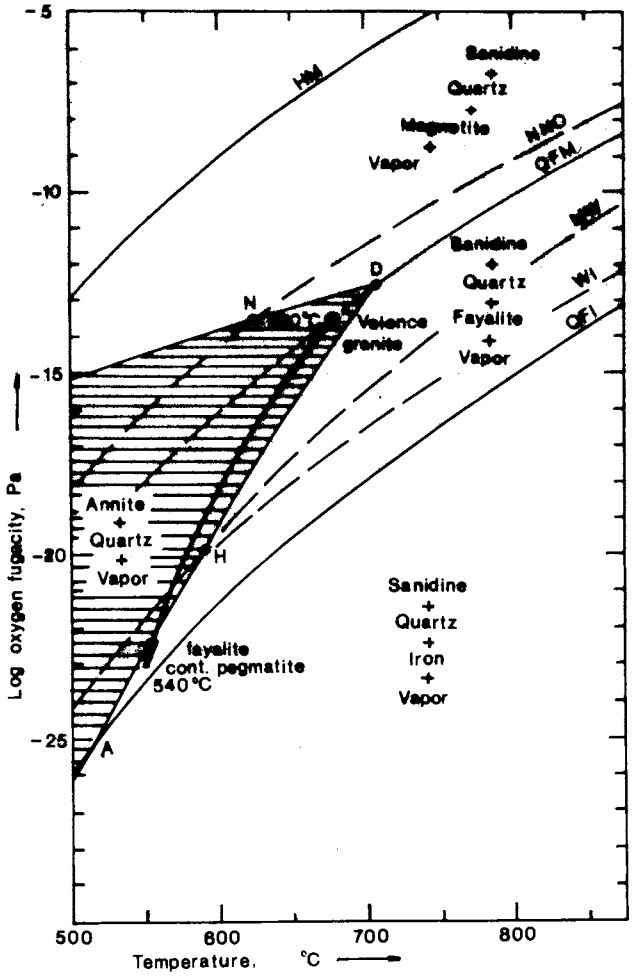

Fig. 11. Phase relations of annite+quartz+vapor, as a function of oxygen fugacity and temperature at 207 MPa pressure (Eugster & Wones, 1962). Arrow shows the dropp of temperature and oxygen fugacity resulting fayalite+K-feldspar+quartz formation instead of annite.

References

Buda Gy., 1981: Genesis of the Hungarian granitoid rocks. *Acta Geol. Acad. Sci. Hung.*, 24, 309 - 318.

Buda Gy., 1985: Origin of collision-type Variscan granitoids in Hungary, West-Carpathian and Central Bohemian Pluton - I, II, Unpublished Ph. D. Thesis (in Hungarian).

Didier J., 1973: Granites and their enclaves. Developments in Petrology - 3. *Elsevier*, 393.

Eugster H. P. & Wones D. R., 1962: Stability relations of the ferruginous biotite, annite. *J. Petrol.*, 3, 82 - 125.

Evans H. T., Appleman D. E. & Handwerker D. S., 1963: The least squares refinement of crystal unit cells with powder diffraction data by an automatic computer indexing method (abst.). *Ann. Meet. Amer. Crystallogr. Soc.*, Cambridge, MA Program, 42 - 63.

Fischer G. W. & Medaris L. G., 1969: Cell dimensions and X-ray determinative curve for synthetic Mg-Fe olivines. *Am. Mineral.*, 54, 741 - 753.

Gatter I. & Molnár F., 1992: Fluid inclusion study of Hungarian granitoids, Part I. (unpublished report), 15.

Haskin L. A., Haskin M. A. & Frey F. A., 1968: In: Ahrens L. H. (Ed.): *Relative and absolute terrestrial abundances of the rare earths in "Origin and Distribution of the Elements." Pergamon Press*, 889 - 912.

Heninger S. G., 1984: Hydrothermal experiments on the andalusite-sillimanite equilibrium. M. Sc. Paper, the Pennsylvania State Univ., 42.

Holdaway M. J., 1971: Stability of andalusite and the aluminium silicate phase diagram. *Am. J. Sci.*, 271. 97 - 131.

Jaeger J. C., 1957: The temperature in the neighbourhood of a cooling intrusive sheet. *Am. J. Sci.*, 255, 306 - 318.

Jaeger J. C., 1961: The cooling of irregularly shaped igneous bodies. *Am. J. Sci.*, 259, 721 - 734.

Jaeger J. C., 1964: Thermal effects of intrusions. *Rev. Geophys.*, 2(3), 443 - 446.

Kerrick D. M., 1990: The Al_2SiO_5 polymorphs. *Reviews in Mineralogy*, 22, 406.

Price R. C., 1983: Geochemistry of a peraluminous granitoid suite from North-eastern Victoria, South-eastern Australia. *Geochim. Cosmochim. Acta*, 47, 31 - 42.

Stormer J. C., 1975: A practical two-feldspar geothermometer. *Am. Mineral.*, 60, 667 - 674.

Tuttle O. F. & Bowen N. L., 1958: Origin of granite in the light of experimental studies in the system $NaAlSi_3O_8$- $KAlSi_3O_8$-SiO_2-H_2O. *Geol. Soc. Amer. Mem.*, 74, 1 - 153.

Vendl A., 1914: Geology and petrology of Velence Mts. *M. Kir. Földt. Int. Évkönyve*, 22, 1 - 170 (in Hungarian).

Whitney J. A. & Stormer J. C., 1977: The distribution of $NaAlSi_3O_8$ between coexisting microcline and plagioclase and its effect on geothermometric calculation. *Am. Minearl.*, 62, 687 - 691.

Winkler M. G. F. & Breitbart R., 1978: New aspects of granitic magmas. *N. Jhb. Min. Mh.*, 10, 463 - 480.

Wones D. R. & Eugster H. P., 1965: Stability of biotite: experiment, theory and application. *Am. Mineral.*, 50, 1228 - 1272.

Wones D. R., 1972: Stability of biotite: A reply. *Am. Mineral.*, 57, 316 - 317.

Yoder H. S. & Sahama Th. G., 1957: Olivine X-ray determinative curve. *Am. Mineral.*, 42, 475 - 491.

RARE EARTH MINERALS: CHEMISTRY, ORIGIN AND ORE DEPOSITS

THE NATURAL HISTORY MUSEUM

Mineralogical Society

IUGS UNESCO

This International Conference was held in the Natural History Museum London on 1 and 2 April 1993. It was organized jointly by the Natural History Museum London and the Mineralogical Society of Great Britain and Ireland. It has brought together scientists from all over the world who are interested in rare earth minerals. All aspects of rare earth minerals were covered from their structure and chemistry to their origin, concentration and alteration in all geological environments. One session considered existing and potential ore deposits and aimed to encourage links between academia and industry.

There were three consecutive sessions :

1 Chemistry - including mineralogy, chemistry and structure.
2 Origin - including phase relations, equilibria, stability and mobility.
3 Ore Deposits - including description and interpretation of existing and potential ore deposits and an invited contribution on the needs and future of REE in industry.

The meeting was part of the official programme for IGCP Project 314, "Alkaline and carbonatic magmatism" and IGCP Project 282 "Rare Metal Granitoids". A pre-conference field meeting of Project 282 was held in Cornwall, England to study the hydrothermal phenomena and evolution of the orefield associated with the Southwest England batholiths. The trip included visits to classic localities such as Cligga Head, the St Just area,the St Austell granite and Cornish tin mine with tin-tungsten mineralization.

102 participants from 26 countries presented their results in three keynote lectures, 19 talks and 43 posters including short talks advertising posters.

The conference was accompanied by trade displays and advertising features of the following Companies or Organisations: Cameca, Chapman & Hall, Elsevier, Mineralogical Society of America, Oxford Instruments (Microanalysis Group), P&H Developments and Tracor Europa.

Copies of the Abstract Volume may be obtained from the Department of Mineralogy Natural History Museum, Cromwell Road, London SW7 5BD, U.K.

by Dr. Igor Rojkovič